



# Quantitative characterization of coal properties using bidirectional diffuse reflectance spectroscopy<sup>☆</sup>

Edward A. Cloutis\*

*Department of Geography, University of Winnipeg, 515 Portage Avenue, Winnipeg, Manitoba, Canada R3B 2E9*

Received 10 December 2002; revised 15 April 2003; accepted 29 April 2003; available online 4 July 2003

## Abstract

The 0.3–26  $\mu\text{m}$  (33,000–385  $\text{cm}^{-1}$ ) reflectance spectra of the  $<45 \mu\text{m}$  fractions of a series of coal samples ranging from lignite to anthracite were analyzed in conjunction with compositional information to derive spectral–compositional–structural relationships. The reflectance spectra, particularly in the 1.8–4  $\mu\text{m}$  (5500–2500  $\text{cm}^{-1}$ ) region exhibit a number of absorption features attributable to both the organic and inorganic components. Quantitative spectral–compositional relationships were found which permit the derivation of properties such as aromaticity, total aliphatic, aromatic content, moisture content, volatile content, fixed carbon abundance, fuel ratio, carbon content, nitrogen abundance, H/C ratio, and vitrinite reflectance. In general, all absorption bands become less intense, and overall reflectance decreases with increasing rank.

© 2003 Elsevier Ltd. All rights reserved.

*Keywords:* Coal; Reflectance spectroscopy

## 1. Introduction

Coals are an exceedingly complex arrangement of organic and inorganic materials [1–3]. Consequently, characterization of coals often requires the application of multiple analytical techniques to derive various parameters of interest [3–6]. A variety of optical spectroscopic techniques have been applied to the analysis of coal samples. The spectroscopic technique with the longest history is infrared transmission spectroscopy [7,8]. It has been joined more recently by techniques such as diffuse infrared spectroscopy [9–13], photoacoustic spectroscopy [14–16], micro-infrared spectroscopy [13,17–20] and attenuated total reflection spectroscopy [21], all of which have the advantage of requiring less sample preparation, thus opening up the possibility of incorporating these techniques into process streams for continuous real-time monitoring [22]. Collectively, these studies have shown that a large number of coal properties can be derived using optical spectroscopic techniques [23].

Coal properties which have been shown to be amenable to quantification using infrared transmission and

absorption spectroscopy include functional group abundances [8,23–27], rank [7,28], aliphatic and aromatic hydrogen contents [27,29,30], aliphatic carbon content [17], carbon aromaticities [27,31], maceral composition [32], compositional variations with rank [33], compositional and structural changes accompanying heating [34], and various utilization parameters [35–37]. Similar work has been performed on the characterization of kerogen and organic-bearing shales [38–40].

Diffuse ultraviolet, visible, and infrared spectroscopy has been used to quantify rank [9,10,12,41,42], degree of oxidation [9], degree of carbonization [10], type of hydrogen bonding [12], air oxidation [43–45], for characterization of macerals [46], and for analysis of coal blends [47]. It has also been used to determine water content and calorific value of peat [48] and to determine level of thermal maturity in organic matter [49].

The present study was designed to expand on earlier work in the applications of diffuse reflectance spectroscopy to coal characterization to determine whether various utilization properties [37] are amenable to quantification using reflectance spectroscopy, to search for additional material properties amenable to quantification using this technique, to examine in greater detail the shorter wavelength regions ( $<2.5 \mu\text{m}$  ( $>4000 \text{cm}^{-1}$ )) for

\* Corresponding author. Tel.: +1-204-786-9386; fax: +1-204-774-4134.

E-mail address: [e.cloutis@uwinnipeg.ca](mailto:e.cloutis@uwinnipeg.ca) (E.A. Cloutis).

<sup>☆</sup> Published first on the web via [Fuelfirst.com](http://www.fuelfirst.com)—<http://www.fuelfirst.com>

additional potentially diagnostic spectral features [16,50], and to conduct a systematic spectral reflectance survey of a range of well-characterized coal samples [36,37,51].

Bidirectional reflectance spectroscopy measures the amount of light reflected from a powdered (or solid) sample as a function of wavelength and for some fixed viewing geometry. In contrast to other techniques such as transmission spectroscopy, bidirectional reflectance spectroscopy is simpler to perform [52], yields generally the same quantity of structural and compositional information [11,13,53], and avoids spectral interferences and structural changes which may accompany KBr pellet production for transmission spectroscopy [54]. At its simplest, no sample preparation is required. However, due to the fact that experimental factors such as changes in viewing geometry and particle size variations can affect the derivation of quantitative sample information, reflectance spectroscopy should normally be performed at a fixed viewing geometry for a consistent particle size distribution if the goal is to derive quantitative information for a suite of samples [11]. This is the approach that has been undertaken in the current study. A number of previous studies have demonstrated that bidirectional or diffuse reflectance spectroscopy is capable of providing quantitative information on hydrocarbon-bearing geological materials, for both the organic and inorganic phases [55–59].

## 2. Experimental

A total of 21 coal samples were used in this study. They include eight samples from the Argonne premium coal

sample program [51], and 13 samples from previous studies [36,37]. These samples are described in Table 1. All samples were gently ground by hand using an alumina mortar and pestle and dry-sieved to obtain  $<45\ \mu\text{m}$  grain size fractions for spectral measurements (the effects of varying grain size are discussed in Section 5). A consistent grain size range was chosen in order to minimize the spectrum-altering effects of grain size variations.

Given that coals are heterogeneous, it is expected that many, if not all, of the coal samples would display some variation in properties for replicate samples and splits. In general, only single determinations were apparently made for the various material properties for samples COAL10–22, and in general multiple determinations were made for the various material properties of samples COAL30–37. The analytical data for which replicate analyses are available are provided in Table 1. In the case of C, H, N, and O contents, H/C ratio, and calorific values for samples COAL30–37, the results are an aggregate of analyses conducted at 55 laboratories [51] for which standard deviations are not available. Similarly H/C ratio is based on the aggregate value. The standard deviations are not large enough to appreciably affect the derived spectral–compositional trends. The reflectance spectra were measured at the Reflectance Experiment Laboratory (RELAB) spectrometer facility at Brown University [60, 61]. The bidirectional technique basically involves illuminating the sample with a collimated illumination source at some angle normal to the sample surface ( $i^\circ$ ) and measuring the light reflected from the sample at another angle ( $e^\circ$ ). The interval from 0.3 to 2.6  $\mu\text{m}$  was measured at 5 nm spectral resolution and  $i = 0^\circ$  and  $e = 30^\circ$ , relative to halon [62].

Table 1a  
Coal samples used in this study

Sample ID	Source	Type	Locality
COAL10	ISPG 597/88	Lignite	Bienfait, Saskatchewan, Canada
COAL11	ISPG 601/88	Lignite	Costello, Saskatchewan, Canada
COAL12	ISPG 581/88	Sub-bituminous	Highvale, Alberta, Canada
COAL13	ISPG 587/88	High volatility C bituminous	Coal Valley, Alberta, Canada (Mynheer/Val D'Or seam)
COAL14	ISPG 914/88	High volatility C/B bituminous	Quinsam, British Columbia, Canada (No. 1 seam)
COAL15	ISPG 917/88	High volatility C/B bituminous	Prince Mine, Nova Scotia, Canada (Hub seam)
COAL16	ISPG 99/88	High volatility A bituminous	Phalen Mine, Nova Scotia, Canada (raw coal)
COAL17	ISPG 97/89	High volatility A bituminous	Phalen/Lingan Mine, Nova Scotia, Canada (Phalen/Harbour seam)
COAL18	ISPG 577/88	High volatility A-medium volatility bituminous	Byron Creek, British Columbia, Canada
COAL19	ISPG 579/88	Medium volatility bituminous	Quintette, British Columbia, Canada
COAL20	ISPG 605/88	Medium volatility bituminous	Line Creek, British Columbia, Canada
COAL21	ISPG 589/88	Low volatility bituminous	Smoky River Coalfield, Alberta, Canada (No. 4 seam)
COAL22	ISPG 103/89	Anthracite	Mt. Klappan, British Columbia, Canada
COAL30	APCS #8	Lignite	Beulah Zap seam, North Dakota, USA
COAL31	APCS #2	Sub-bituminous	Wyodak-Anderson seam, Wyoming, USA
COAL32	APCS #3	High volatility bituminous	Illinois # 6 seam, Illinois, USA
COAL33	APCS #6	High volatility bituminous	Blind Canyon seam, Utah, USA
COAL34	APCS #7	High volatility bituminous	Lewiston-Stockton seam, West Virginia, USA
COAL35	APCS #4	High volatility bituminous	Pittsburgh #8 seam, Pennsylvania, USA
COAL36	APCS #1	Medium volatility bituminous	Upper Freeport seam, Pennsylvania, USA
COAL37	APCS #5	Low volatility bituminous	Pocahontas #3 seam, Virginia, USA

Note. ISPG indicates samples obtained from the Geological Survey of Canada's Institute of Sedimentary and Petroleum Geology. APCS indicates samples from the Argonne Premium Coal Sample Program. Compositional data for these samples can be found in Refs. [36,37,51].

Table 1b  
Compositional properties of coal samples used in this study [51]

Sample ID	Aromaticity factor	Standard deviation (number of measurements)	Moisture content	Standard deviation	Volatile content	Standard deviation
COAL30	0.69	0.05 (12)	32.24	0.8672	30.45	2.4189
COAL31	0.62	0.04 (11)	28.09	0.7043	32.17	1.2241
COAL32	0.71	0.02 (10)	7.97	0.0656	36.86	0.7566
COAL33	0.63	0.03 (11)	4.63	0.1215	43.72	0.8061
COAL34	0.75	0.02 (9)	2.42	0.1990	29.44	0.3539
COAL35	0.72	0.03 (11)	1.65	0.1094	37.20	0.4274
COAL36	0.80	0.02 (10)	1.13	0.0725	27.14	0.5156
COAL37	0.85	0.01 (12)	0.65	0.1111	18.48	0.6508
Sample ID	Fixed carbon content	Standard deviation	Mean vitrinite reflectance	Standard deviation (number of measurements)		
COAL30	30.7	3.4153	0.28	0.04 (49)		
COAL31	33.0	2.0377	0.31	0.08 (50)		
COAL32	40.9	1.0850	0.46	0.05 (24)		
COAL33	52.8	1.0399	0.50	0.05 (50)		
COAL34	52.2	0.6749	0.77	0.05 (50)		
COAL35	52.0	0.7193	0.72	0.04 (50)		
COAL36	58.7	0.7390	0.99	0.07 (50)		
COAL37	76.1	0.8314	1.42	0.06 (50)		

*Note.* Fixed carbon content taken as the remainder after subtracting moisture, ash, and volatile contents. Standard deviations taken as the sum of the standard deviations for moisture, ash, and volatile contents. The standard deviation in fuel ratio (not listed) which is the ratio of fixed carbon to volatile matter can also be determined from the standard deviations for the constituent determinations.

The interval from 1.8 to 26  $\mu\text{m}$  was measured at  $4\text{ cm}^{-1}$  spectral resolution and  $i = 30^\circ$  and  $e = 30^\circ$  relative to brushed gold. The spectra were also corrected for minor ( $\sim 2\%$ ) irregularities in halon's absolute reflectance in the 2- $\mu\text{m}$  region and dark current offsets. The two sets of spectra were merged in the 1.8–2.6  $\mu\text{m}$  region. The sample spectra were measured in an environment chamber under dry air conditions. No additional attempt was made to purge the samples of adsorbed water, for instance, as it was felt that additional sample processing might inadvertently alter the composition of the samples, and the desire was to examine the spectral reflectance properties of 'raw' samples. This approach probably results in enhancements of the depths of  $\text{H}_2\text{O}$ -associated absorption bands due to the adsorbed component, some of which would be removed by exposing the samples to the dry air environment.

The wavelength positions of absorption bands were determined by fitting a third order polynomial equation to between 10 and 20 data points on either side of a visually determined minimum or center. Absorption bands for which no continuum removal was applied are termed band minima. In some cases absorption bands were isolated by dividing the spectrum by a straight-line continuum tangent to the reflectance spectrum on either side of an absorption feature of interest. The wavelength position of minimum reflectance of features isolated in this way are referred to as band centers. Absorption band depths were measured

using Eq. (32) of Clark and Roush [63] relative to these continua.

### 3. Reflectance spectra of coals

The reflectance spectra of some of the coal samples used in this study over the interval 0.3–26  $\mu\text{m}$  are shown in Figs. 1–3. In the 0.3–2.6  $\mu\text{m}$  region (Fig. 1), distinct

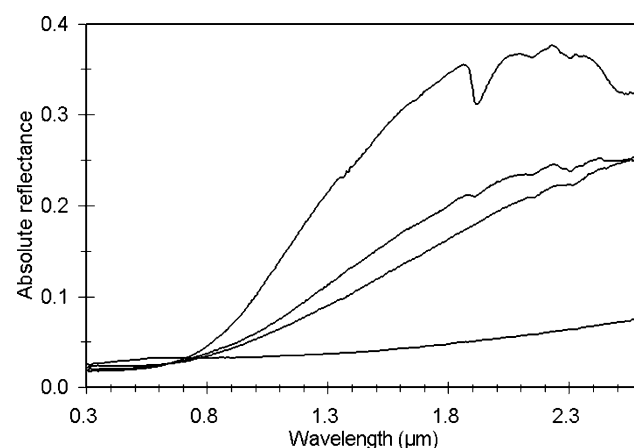


Fig. 1. Reflectance spectra (0.3–2.6  $\mu\text{m}$ ) of a number of coal samples. From top to bottom at 2  $\mu\text{m}$ : COAL10 (lignite), COAL14 (high volatility C/B bituminous), COAL21 (low volatility bituminous), and COAL22 (anthracite).

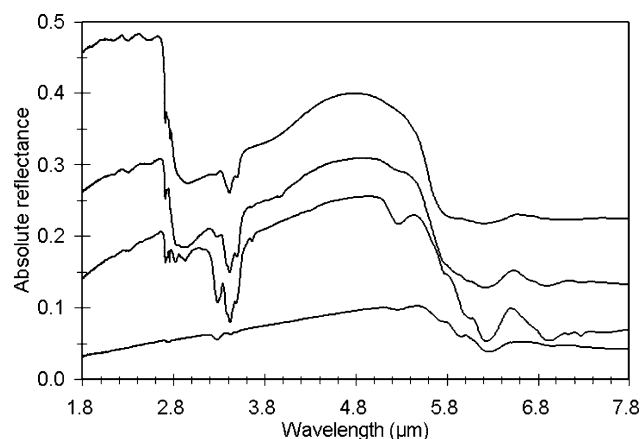


Fig. 2. Reflectance spectra (1.8–7.8  $\mu\text{m}$ ) of a number of coal samples. From top to bottom: COAL10 (lignite, vertically offset by +0.2 for clarity), COAL14 (high volatility C/B bituminous; vertically offset by +0.1 for clarity), COAL21 (low volatility bituminous, no vertical offset), and COAL22 (anthracite, no vertical offset).

absorption bands generally only appear in the lowest ranked samples, in the 1.4, 1.9 and 2.1–2.6  $\mu\text{m}$  regions, and generally diminish in intensity with increasing rank. The 1.4 and 1.9  $\mu\text{m}$  features are associated with free, bonded, and/or adsorbed water [16,64]. Absorption bands in the 2.1–2.6  $\mu\text{m}$  region can be attributed to metal-OH overtones in clays as well as combinations and overtones of C–H fundamentals [56,64,65]. Weaker bands are also sometimes present in the 1.7 and 2.3–2.5  $\mu\text{m}$  region. The 1.7  $\mu\text{m}$  region bands are weak, on the order of  $<1\%$  depth; they are first order overtones and combinations of the various aliphatic C–H stretching fundamentals [50,56]. They are generally difficult to resolve [17]. Absorption bands in the 2.3  $\mu\text{m}$  region can be assigned to either various organic combination and overtone bands [56] and/or OH-associated clay absorption bands [66]. Band depths in this region for the samples used in this study do not exceed 6%.

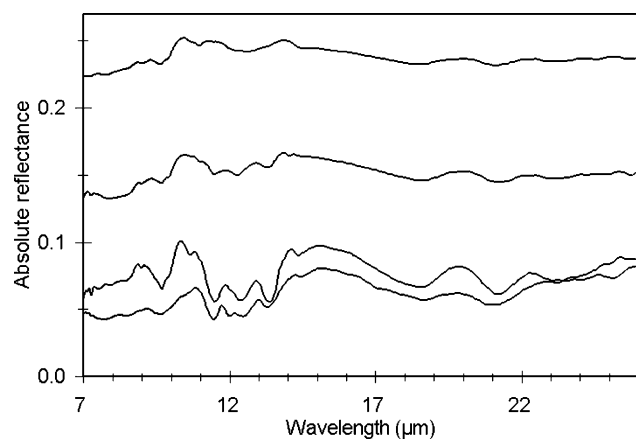


Fig. 3. Reflectance spectra (7–26  $\mu\text{m}$ ) of a number of coal samples. From top to bottom: COAL10 (lignite, vertically offset by +0.2 for clarity), COAL14 (high volatility C/B bituminous; vertically offset by +0.1 for clarity), COAL21 (low volatility bituminous, no vertical offset), and COAL22 (anthracite, no vertical offset).

The major spectral differences in the 0.3–2.6  $\mu\text{m}$  region coal spectra relate to the overall spectral shape. With increasing rank, overall reflectance generally decreases and the spectra become flatter [67]. This is due to the fact that increasing aromatization results in the absorption edge due to electronic transitions in aromatic molecules moving to longer wavelengths [10,16,31,41,64,68]. It has been found that the intensity of absorption in the 1.6  $\mu\text{m}$  region is a function of fixed carbon and inertinite content [10].

In the 1.8–7.8  $\mu\text{m}$  region, coal reflectance spectra are dominated by a series of absorption bands in the 2.7–3.5  $\mu\text{m}$  region and a broader region of absorption in the 5.6–6.6  $\mu\text{m}$  region (Fig. 2). The absorption bands in the 2.7–3.0  $\mu\text{m}$  region are attributable to bound and adsorbed water [65,66]. The fine structure evident in some of the coal spectra in this region can be attributed to various distinct types of OH bonding [69]. Even small amounts of OH (on the order of 0.1% OH) can give rise to absorption bands in this region [70].

The 3.2–3.5  $\mu\text{m}$  region is characterized by absorption bands attributable to aromatic C–H stretches (at 3.28  $\mu\text{m}$ ) and  $\text{CH}_2$  and  $\text{CH}_3$  stretching fundamentals (in the 3.4–3.5  $\mu\text{m}$  region) [8,24,25]. Increasing rank (and hence aromatization) leads to an increase in the depth of the aromatic band near 3.28  $\mu\text{m}$  relative to the aliphatic bands in the 3.4–3.5  $\mu\text{m}$  region. The 5.6–6.6  $\mu\text{m}$  region is more complex. Candidate absorptions include an H–O–H bend, carbonyl and carboxylic groups, and aromatic ring stretches [8,24,66]. The precise assignments of absorption bands in this region have been the subject of numerous studies in the past [24]. The longer wavelength regions ( $>7\ \mu\text{m}$ ) are characterized by low overall reflectance (Fig. 3). Distinct absorption bands are generally only found in the 11–14, 18.5, and 21  $\mu\text{m}$  regions. The bands in the 11–14  $\mu\text{m}$  region are attributable to aromatic C–H out-of-plane bends [24], and these become more prominent with increasing rank and aromatic content. Bands in the 16–25  $\mu\text{m}$  ( $400\text{--}600\ \text{cm}^{-1}$ ) region have generally been assigned to various mineral absorption bands [8,29,71].

#### 4. Spectral–compositional correlations

In general, reflectance spectra provide much the same structural and compositional information as transmission spectra. Thus, we expect the quality and quantity of information which might be derived from reflectance spectra to be roughly comparable to that available from transmission spectra. The ensuing discussion emphasizes the shortest wavelength spectral–compositional correlations which are found.

In terms of deriving correlations, as discussed below, some of the sample properties appear to be strongly correlated with spectral parameters. The trends which have been found are of variable quality and utility. The intent of this study was to provide a survey of the potential

utility of bidirectional reflectance spectroscopy for coal characterization rather than to develop rigorous quantitative correlations at this stage.

#### 4.1. Aromaticity factor

The aromaticity factor ( $f_a$ ) is defined as the ratio of protonated and non-protonated aromatic carbon atoms relative to total carbon (normally derived from FTIR or  $^{13}\text{C}$  NMR spectroscopy) [24,27,37,72]. Given that this is a ratio, some of the difficulties inherent in proper sample preparation for quantitative analysis (particularly for FTIR analysis) can be minimized [24,73]. As described above, the aromatic C–H stretching absorption band is present at 3.28  $\mu\text{m}$ , and the aliphatic fundamental bands are present in the 3.4–3.5  $\mu\text{m}$  region (with overtone and combination bands in the 1.7 and 2.3  $\mu\text{m}$  regions). Thus, we expect aromaticity to be positively correlated with band depth at 3.28  $\mu\text{m}$  and negatively correlated with aliphatic band depths. These correlations are in fact present; however, anthracite exhibits lower than expected

band depths, probably due to its low overall reflectance. The strongest correlations with aromaticity are found with the depth of the aliphatic absorption feature at 3.41  $\mu\text{m}$  (as measured relative to the local reflectance maximum near 2.25  $\mu\text{m}$ ), as well as with the ratio of the 3.28–3.41  $\mu\text{m}$  band depths (Fig. 4).

#### 4.2. Aliphatic ( $\text{CH}_3$ ) or ( $\text{CH}/\text{CH}_2$ ) abundances

Aliphatic groups are expressed in the reflectance spectra in the 1.7, 2.3 and 3.4–3.5  $\mu\text{m}$  regions. Painter et al. [25] discussed in depth the difficulties inherent in deriving absolute abundances of aliphatics from analysis of transmission spectra. A search for correlations between the reflectance spectra and  $\text{CH}_3$  or  $\text{CH} + \text{CH}_2$  abundances failed to yield any strong correlations. One reason for this lack of correlation may be that the organic absorption bands in the 1.7, 2.3 and 3.4–3.5  $\mu\text{m}$  regions are composed of multiple overlapping bands which does not allow for sufficient discrimination of  $\text{CH}_3$ - versus  $\text{CH}_2$ - versus  $\text{CH}$ -associated absorption bands.

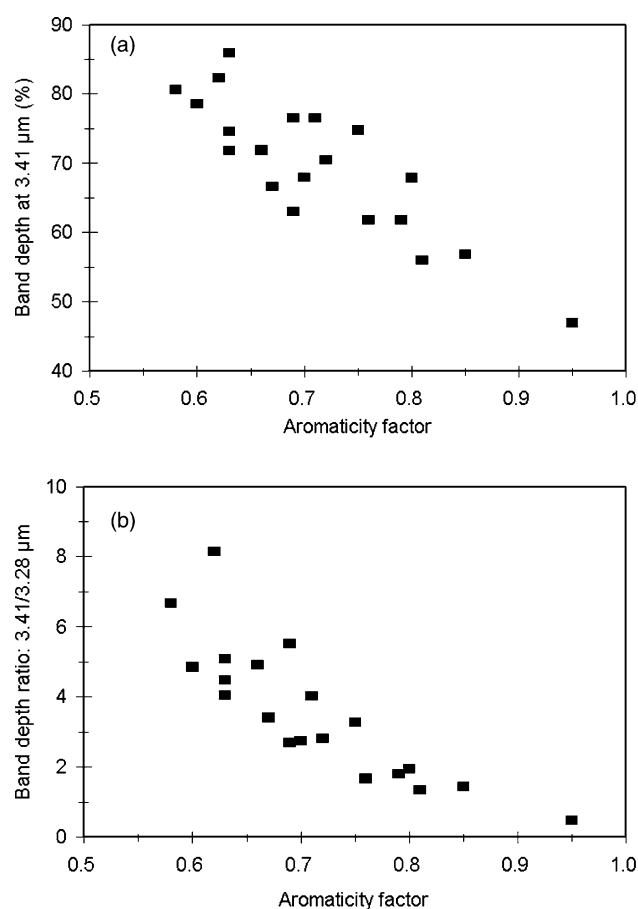


Fig. 4. Aromaticity factor ( $f_a$ ) versus: (a) depth of absorption band at 3.41  $\mu\text{m}$  measured relative to the local reflectance maximum in the 2.5–2.7  $\mu\text{m}$  region; (b) ratio of the depths of the 3.41/3.28  $\mu\text{m}$  absorption bands measured relative to a straight line continuum tangent to the reflectance spectra on either side of these features.

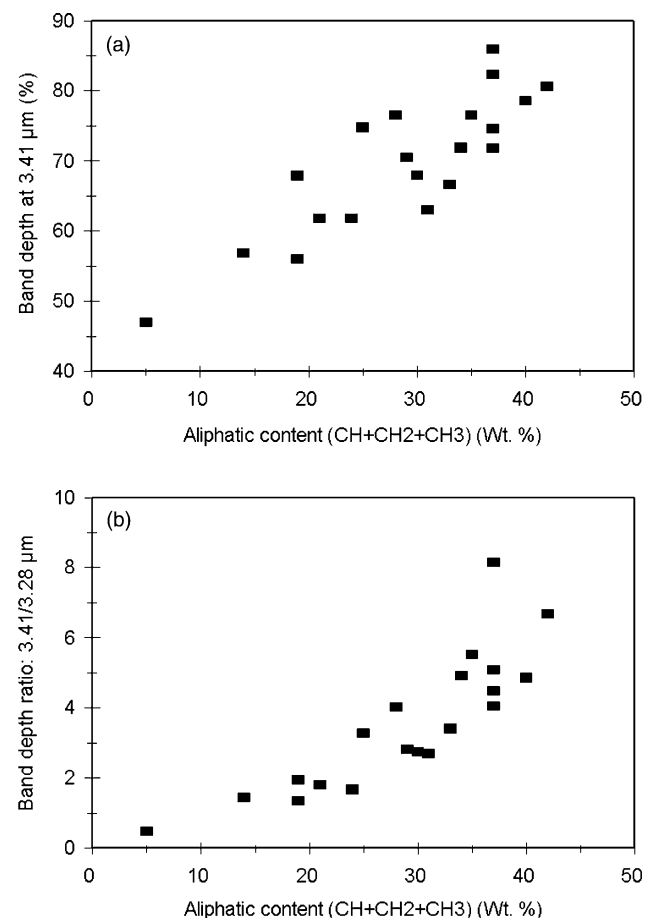


Fig. 5. Total aliphatic content ( $\text{CH} + \text{CH}_2 + \text{CH}_3$ ) versus: (a) depth of absorption band at 3.41  $\mu\text{m}$  measured relative to the local reflectance maximum in the 2.5–2.7  $\mu\text{m}$  region; (b) ratio of the depths of the 3.41/3.28  $\mu\text{m}$  absorption bands measured relative to a straight line continuum tangent to the reflectance spectra on either side of these features.

#### 4.3. Total aliphatic (CH/CH<sub>2</sub>/CH<sub>3</sub>) abundance

When total aliphatic groups (CH + CH<sub>2</sub> + CH<sub>3</sub>) are considered, a number of useful correlations with spectral reflectance properties appear. The best correlations exist between total aliphatic abundance and depth of the absorption feature at 3.41 μm (as measured relative to the local reflectance maximum near 2.25 μm), and the ratio of the 3.41–3.28 μm band depths (Fig. 5). These relationships are not unexpected as all of the spectra were measured for <45 μm grain size fractions, thereby minimizing the effects of grain size variations. Good correlations were also found between total aliphatic content and depth of the 2.31 μm feature, absolute reflectance at 1.6 and 2.31 μm, depth of the aromatic band at 3.28 μm (with the exception of anthracite), and difference in band depth between the 3.41 and 2.31 μm bands. These correlations are also expected given the mechanisms leading to absorptions in the 2.31 and 3.41 μm regions and the fact that absolute reflectance generally decreases with increasing aromatic (and decreasing aliphatic) content [73]. Microspectroscopy was found to be incapable of measuring aliphatic content in individual macerals due to high light scattering and low absorption in the 1.7 μm region [17]. The 1.7 μm region has also been found to be less suitable than the 2.31 and 3.41 μm regions in the macroscopic study because of the weakness of absorption bands in this region (Fig. 1).

#### 4.4. Aromatic (C=C) abundance

Changes in aromatics abundance are expected to most directly affect overall reflectance as well as the depth of the aromatic-associated 3.28 μm band. The latter relationship is due to the fact that increasing aromatics abundance shifts the absorption edge to progressively longer wavelengths and reduce overall reflectance [10,16,41,64,68]. While a weak negative correlation was found between overall reflectance at selected wavelengths and aromatic abundance, the best correlations which were found relate aromatic content to the depth of the 3.28 μm band (relative to the 3.41 μm aliphatic band) and the ratio of the depth of the 3.28 μm aromatic band to its absolute reflectance (Fig. 6). In addition, the aromatic absorption bands in the 11–13 μm region all exhibited weak positive correlations with aromatic content, but were not as well constrained as those involving exhibited greater scatter than those in the 3.28 μm region.

#### 4.5. Vitrinite, inertinite, liptinite abundances

No strong correlations were found between spectral properties and major maceral types (vitrinite, inertinite, liptinite abundances). This is not unexpected, as maceral types are based more on morphological than compositional criteria. The only weak correlation was found was between absolute reflectance of the 3.41 μm absorption band and inertinite content (positive correlation). The expected

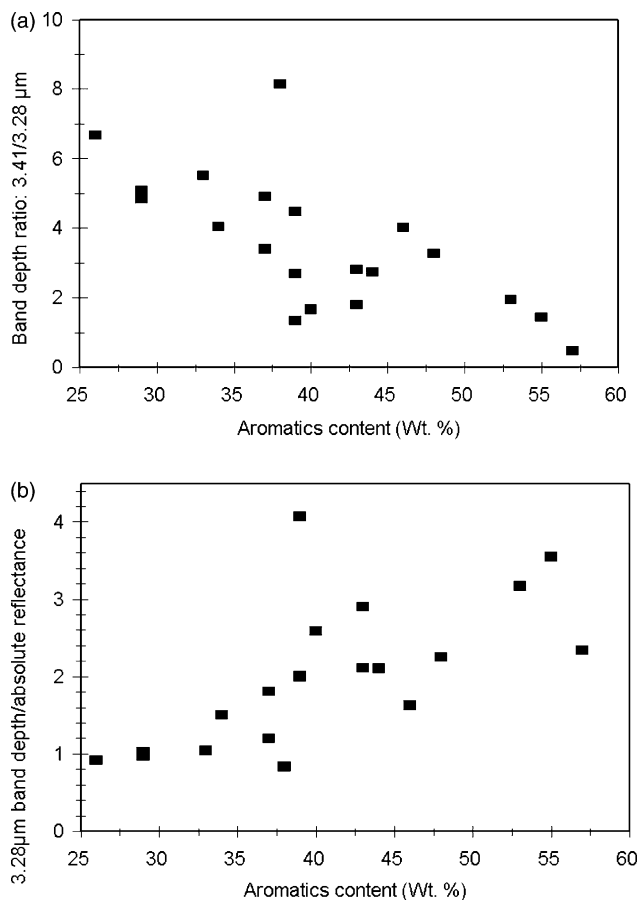


Fig. 6. Aromatic content versus: (a) depth of absorption band at 3.28 μm measured relative to a straight line continuum tangent to the reflectance spectra on either side of this feature; (b) depth of absorption band at 3.28 μm (measured relative to a straight line continuum tangent to the reflectance spectrum on either side of this feature) divided by the absolute reflectance of this band.

correlation found between inertinite content and reflectance at 1.6 μm [10] was also found but too much scatter is present in the data to allow this relationship to be used to reliably predict inertinite content.

#### 4.6. Moisture content

Moisture in coals may be present in a number of forms including structural water (OH), adsorbed, or free water. Each of these forms will be expressed in unique ways in reflectance spectra [66,74]. In the absence of sophisticated spectral deconvolution algorithms, simple spectral parameters may not accurately represent the total moisture content and would not capture the full information content concerning water types which are inherent in the spectra. Even simple measures of band depths, however, do provide a reasonably accurate measure of moisture content for the samples studied. Strong positive correlations were found between moisture content and absorption band depths at 1.9 and 2.95 μm. The 1.9 μm band is attributable to a combination of an O–H stretch and H–O–H bend. Thus this band is only present when

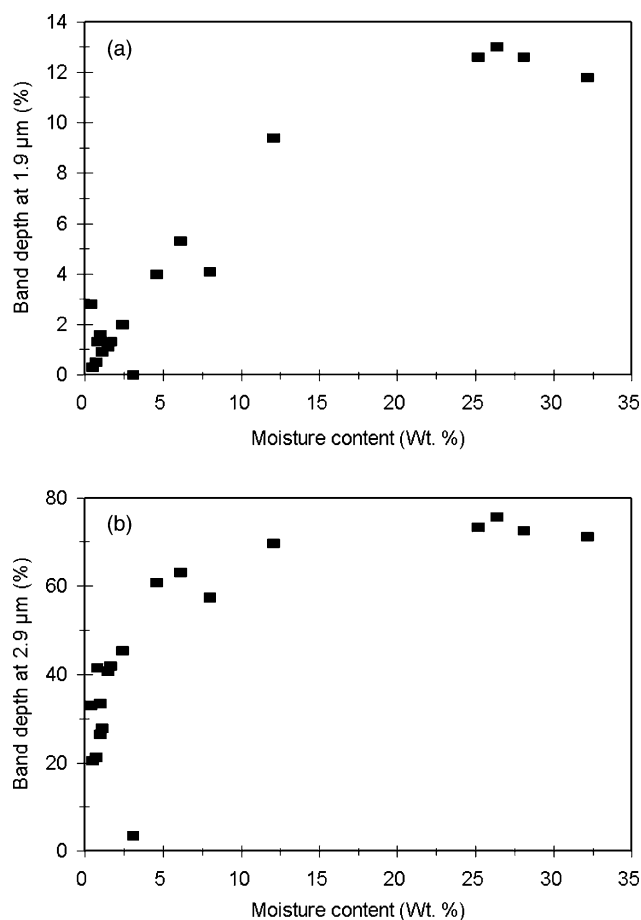


Fig. 7. Moisture content versus: (a) depth of absorption band in the 1.9  $\mu\text{m}$  region measured relative to a straight line continuum tangent to the reflectance spectra on either side of this feature; (b) depth of the absorption feature in the 2.9  $\mu\text{m}$  region measured relative to the local reflectance maximum in the 2.5–2.7  $\mu\text{m}$  region.

the sample contains  $\text{H}_2\text{O}$  molecules as opposed to OH. The correlation which exists between the depth of this band and moisture content suggests that much of the moisture is present as  $\text{H}_2\text{O}$  (Fig. 7). In the 2.95  $\mu\text{m}$  region, the coal samples with the highest moisture contents exhibit spectra which are characterized by a broad and relatively featureless absorption band in this region (Fig. 2). The depth of this feature is also correlated with moisture content (Fig. 7). Given that the 1.9  $\mu\text{m}$  band is a combination band, its depth is not nearly as great as for the 2.95  $\mu\text{m}$  band; its depth increases gradually with moisture content and peaks near 14%. The 2.95  $\mu\text{m}$  band, being a fundamental band, is much stronger, and band depth increases very rapidly over the first few weight percent moisture, peaking around 75% band depth. With decreasing moisture content, band depths at 2.9  $\mu\text{m}$  decrease and more spectral structure (i.e. more resolvable absorption bands), attributable to specific minerals appear (Fig. 2).

All of the spectra exhibit additional narrow absorption bands in the 2.7–2.9  $\mu\text{m}$ . These bands are attributable to the various clay minerals which are present in the samples and which normally make up the bulk of the mineral matter in

coals [51,75]. The wavelength positions of the various bands could be used to distinguish the different clay minerals [66].

#### 4.7. Ash content

Ash content refers to the abundance of material remaining after combustion and includes organo-metallic components (minor) and inorganics such as clays, pyrite, and quartz (major) [51]. Given that ash content is non-specific in terms of associated spectral characteristics, no correlations are expected (or were found) between the coal spectra and ash content. A lack of correlation is not unexpected given the diversity of mineral types which are found in coals and the variations in mineralogy that may accompany rank [76]. Nevertheless, infrared spectroscopy can be used to identify and quantify the abundances of various minerals in coals [77].

#### 4.8. Volatile content

Volatile content refers to the material lost upon combustion (after drying) and is generally equated with the organic (hydrocarbon-bearing) fraction. Thus it is in many ways comparable to the aliphatic content in terms of expected spectral correlations. The best correlations found relate volatile content to the depths of the 2.31 and 3.41  $\mu\text{m}$  absorption bands as well as the ratio of the 3.41/3.28  $\mu\text{m}$  absorption band depths (Fig. 8).

#### 4.9. Fixed carbon content

Fixed carbon content is defined here as the non-volatile matter in coal minus the ash. More precisely fixed carbon is the product of pyrolysis under some set of standard conditions. Because of the fact that the carbon samples derived from different sources, the definition of fixed carbon as defined here was used to enable intercomparison of the samples. Spectrally, it is expected that fixed carbon should be similar to aromatic carbon as fixed carbon is correlated with aromaticity [78]. This is in fact the case. The best spectral correlations for fixed carbon content involve the depth of the 3.41  $\mu\text{m}$  aliphatic absorption band (inverse correlation), the ratio of the 3.41/3.28 aromatic/aliphatic band depth ratio, and the ratio of the 3.28  $\mu\text{m}$  band depth to its absolute reflectance (Fig. 9). Ito et al. [10] found that reflectance at 1.6  $\mu\text{m}$  was inversely correlated with carbon content. A similar relationship was found in this study, but the scatter in the data precludes the use of this relationship for more than broad categorization of fixed carbon content. It was found to be not as well constrained exhibit a higher degree of scatter compared to the other spectral parameters.

#### 4.10. Fuel ratio

Fuel ratio is defined here as the ratio of fixed carbon to volatile matter [36,79]. This ratio is dependent on

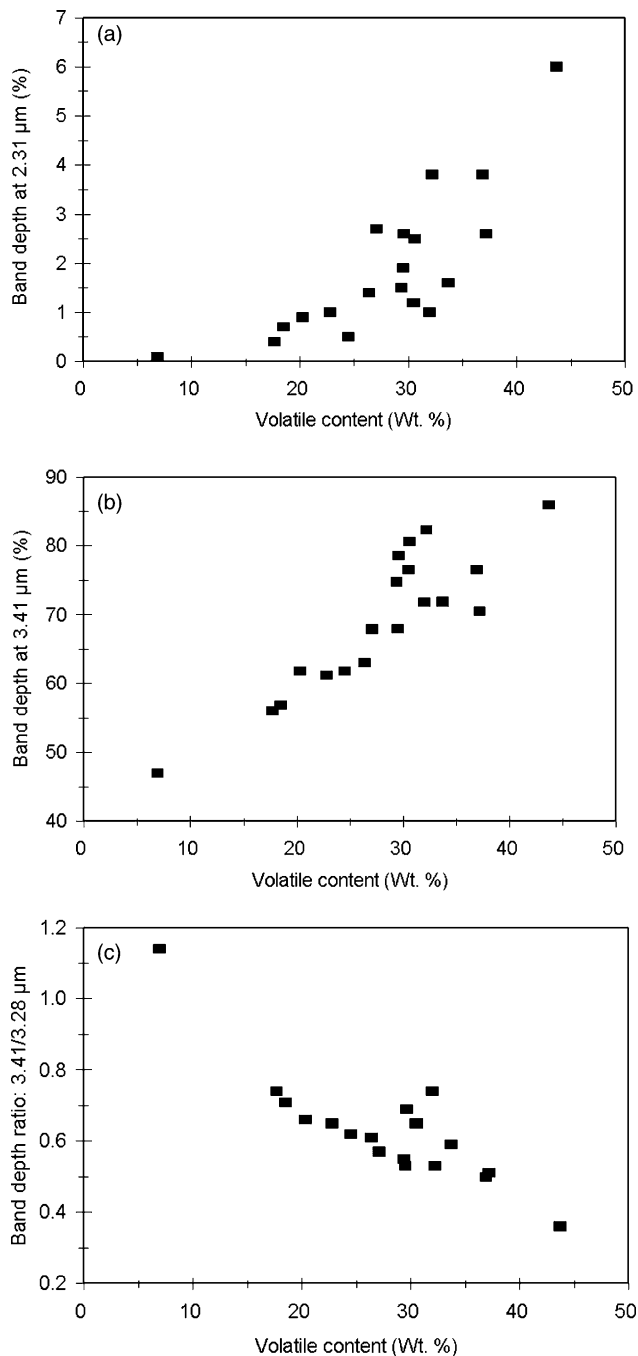


Fig. 8. Volatile content versus: (a) depth of absorption band at 2.31 μm measured relative to the local reflectance maximum near 2.25 μm; (b) depth of the absorption band at 3.41 μm measured relative to the local reflectance maximum in the 2.5–2.7 μm region; (c) ratio of the depths of the 3.41/3.28 μm absorption bands measured relative to a straight line continuum tangent to the reflectance spectra on either side of these features.

the spectral properties associated with both volatile matter and fixed carbon. Given that both fixed carbon and volatile matter contents can be derived from associated spectral variations, fuel ratio is derivable from the variations in the coal reflectance spectra. The best correlation for fuel ratio involves ratios of aromatic (3.28 μm) and aliphatic (3.41 μm) band depths (Fig. 10). As can be seen in

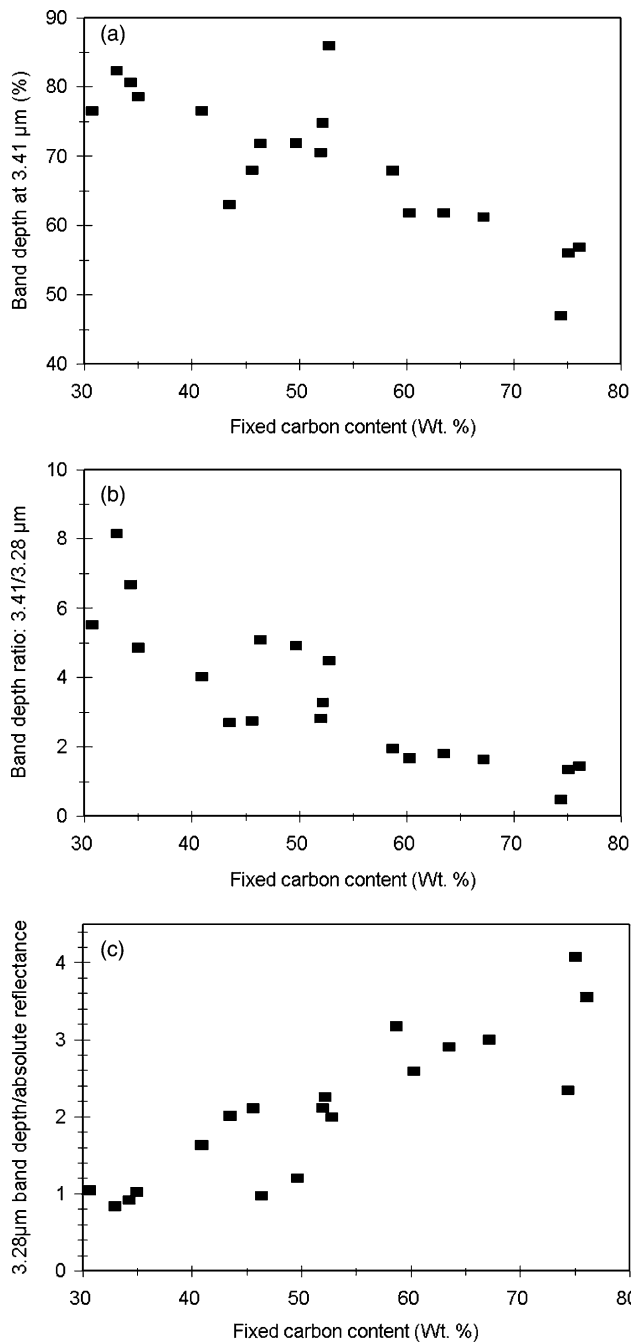


Fig. 9. Fixed carbon content versus: (a) depth of absorption band at 3.41 μm measured relative to the local reflectance maximum in the 2.5–2.7 μm region; (b) ratio of the depths of the 3.41/3.28 μm absorption bands measured relative to a straight line continuum tangent to the reflectance spectra on either side of these features; (c) depth of the absorption band at 3.28 μm (measured relative to a straight line continuum tangent to the reflectance spectrum on either side of this feature) divided by the absolute reflectance of this band.

Fig. 10, for the 3.41/3.28 μm band depth ratio, when the fuel ratio is less than ~2, the band depth ratio cannot be used to constrain its value. This is probably attributable to the fact that the 3.41 μm absorption band is probably quite close to saturation for the samples with the highest volatile matter content. This is borne out by the fact that using the

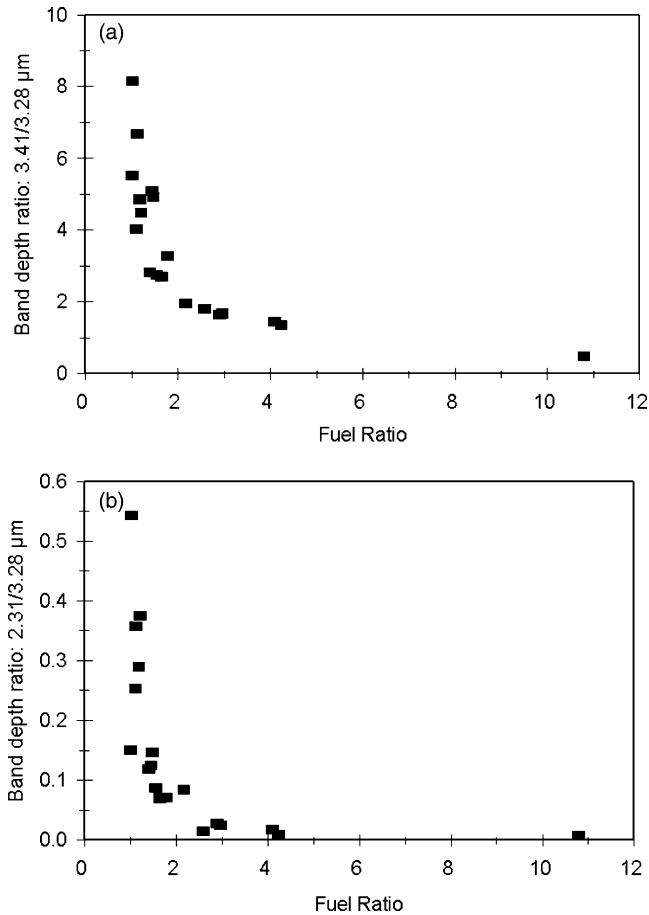


Fig. 10. Fuel ratio versus: (a) ratio of the depths of the 3.41/3.28  $\mu\text{m}$  absorption bands measured relative to a straight line continuum tangent to the reflectance spectra on either side of these features; (b) ratio of the depths of the 2.31/3.28  $\mu\text{m}$  absorption bands (the depth of the 2.31  $\mu\text{m}$  absorption band is measured relative to the local reflectance maximum near 2.25  $\mu\text{m}$  and the depth of the 3.28  $\mu\text{m}$  absorption band is measured relative to a straight line continuum tangent to the reflectance spectra on either side of this band).

2.31  $\mu\text{m}$  absorption band in the ratio (2.31/3.28  $\mu\text{m}$ ) allows for discrimination of fuel ratios as low as  $\sim 1$  (Fig. 10).

#### 4.11. Carbon (wt%)

In contrast to proximate analyses, ultimate analyses are less sensitive to structural properties of coals. There are a number of confounding factors which probably impede the derivation of widely applicable and reliable spectral–elemental correlations. However, given that composition and structure are often related (e.g. a high C content, or C/H ratio would imply a higher rank), some elemental information may be derivable from the reflectance spectra. These results should be used with caution as they may only be strictly applicable to the types of coals included in this analysis. Gilbert [41] found that the carbon content of coal vitrains could be distinguished on the basis of reflectance

below  $\sim 0.5 \mu\text{m}$ . However for whole coal samples, while overall reflectance at 0.4  $\mu\text{m}$  increased with increasing carbon content, the correlation was not strong enough to permit its use as a reliable predictive tool. For the whole coal sample spectra used in this study, correlations were found between carbon content and the depth of the 3.41  $\mu\text{m}$  aliphatic band (negative correlation), absolute reflectance at 1.6  $\mu\text{m}$  (negative correlation), the ratio of the 3.41/3.28  $\mu\text{m}$  band depths (negative correlation), and the ratio of the 3.28  $\mu\text{m}$  band depth to its absolute reflectance (positive correlation). Of these, the latter two are the most highly correlated and hence most useful for predicting carbon content (Fig. 11). Reflectance at 1.6  $\mu\text{m}$  was also found to be negatively correlated with carbon content by Ito et al. [10].

#### 4.12. Hydrogen (wt%)

As was the case for carbon content, few well-defined correlations exist between the coal reflectance spectra and hydrogen content. The best correlation which was found is

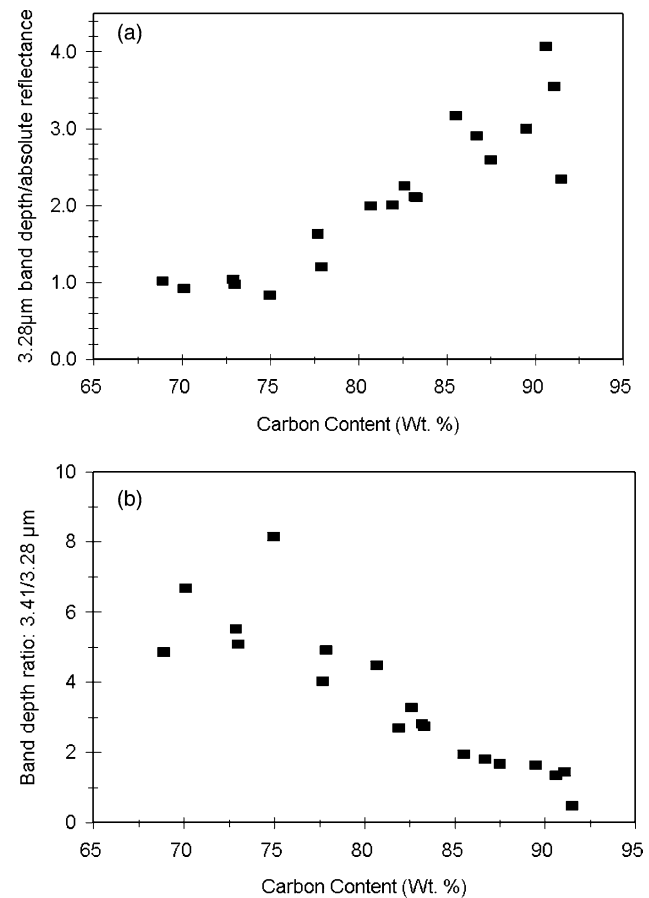


Fig. 11. Carbon content versus: (a) depth of the absorption band at 3.28  $\mu\text{m}$  (measured relative to a straight line continuum tangent to the reflectance spectrum on either side of this feature) divided by the absolute reflectance of this band; (b) ratio of the depths of the 3.41/3.28  $\mu\text{m}$  absorption bands measured relative to a straight line continuum tangent to the reflectance spectra on either side of these features.

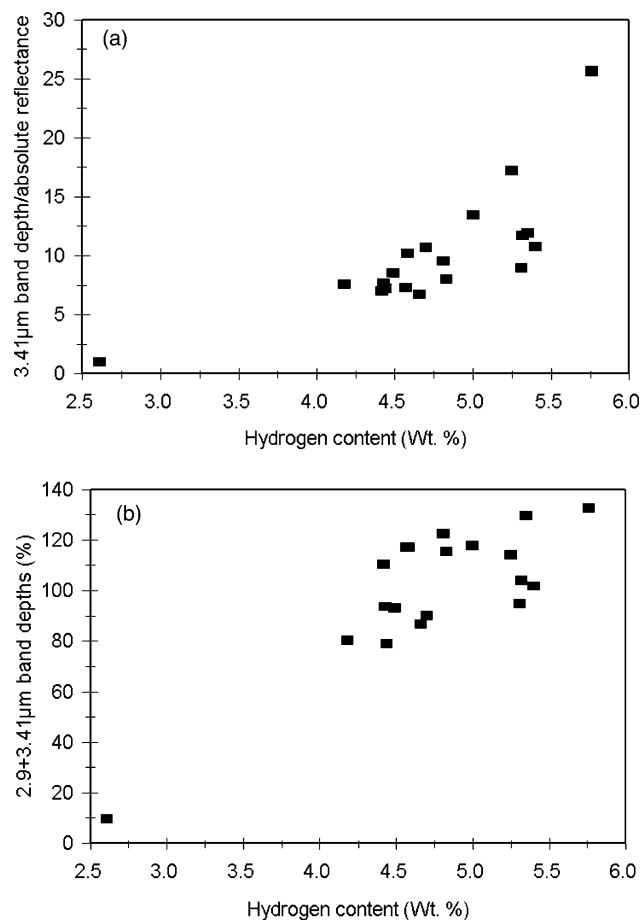


Fig. 12. Hydrogen content versus: (a) ratio of the depth of the 3.41 μm absorption band (measured relative to a straight line continuum tangent to the reflectance spectrum on either side of this band) to the absolute reflectance of this feature; (b) sum of the band depths at 2.9 μm (measured relative to the local reflectance maximum in the 2.5–2.7 μm region) and at 3.41 μm (measured relative to a straight line continuum tangent to the reflectance spectrum on either side of this feature).

between hydrogen content and the ratio of band depth to absolute reflectance of the aliphatic 3.41 μm absorption band, as well as the sum of the 2.9 and 3.41 μm absorption bands (Fig. 12). As was the case with the carbon ratio, hydrogen can be present in a variety of forms in coal, therefore use of these correlations should be undertaken cautiously. Infrared transmission spectroscopy can be used to study the various forms of hydrogen bonding which occur in coals [12,29,69].

#### 4.13. Nitrogen (wt%)

Nitrogen contents in coal are generally low (<1%) and nitrogen content has not been found to be correlated with rank [79]. Nitrogen-associated absorption bands are expected in the 3.0–3.3 μm (due to N–H stretches), 6.2–6.6 μm (due to N–H bends), and 7.1–7.4 μm region (due to C–N stretches) [80]. The only resolvable candidate absorption band which was found to correlate with nitrogen content

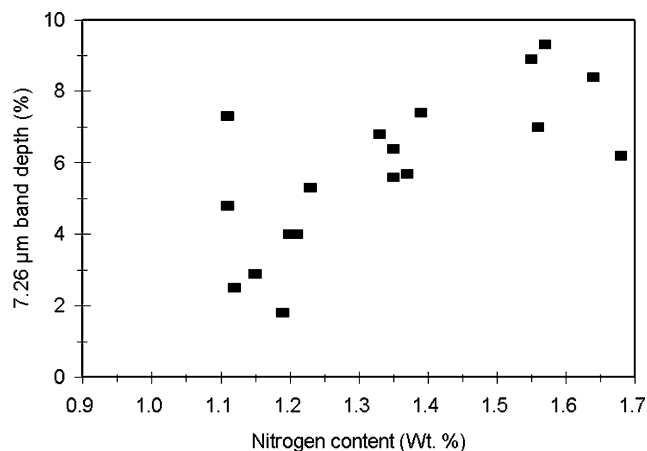


Fig. 13. Nitrogen content versus depth of the absorption band at 7.26 μm measured relative to a straight line continuum tangent to the reflectance spectrum on either side of this feature.

appears at 7.26 μm (Fig. 2). There is a weak positive correlation between N content and depth of this band (Fig. 13) suggesting that it is in fact a C–N stretching band. Its depth is uncorrelated with other elemental abundances. The scatter in the data suggests that nitrogen is probably present in a variety of forms; i.e. bound to other atoms besides C, as expected. However, it appears to be useful for placing gross constraints on nitrogen content, under the assumption that C–N is the major bonding mechanism. Partial least squares regression analysis has been used to correlate changes in spectral properties with the nitrogen content of peat [35].

#### 4.14. Oxygen (wt%)

Fuller et al. [9] used the intensity of an absorption band at 5.83 μm (1715 cm<sup>-1</sup>), attributable to carbonyl, to determine degree of oxidation of coals. This band occurs on the wing of the intense 1600 cm<sup>-1</sup> 6.25 μm (1600 cm<sup>-1</sup>) general absorption feature which is attributable to a number of absorption mechanisms [25]. A reliable mechanism for isolating this band in the reflectance spectra to determine actual band depths could not be found. However, positive correlations were found with as-received water content and overall oxygen content (on both a moisture and ash-free, and a dry and mineral matter-free basis, as well as with total oxygen by difference) with the depths of the 1.9 and 2.9 μm bands (Fig. 14). Strong correlations were also found between all combinations of the as-received water contents and the various oxygen abundance determinations. Given that much of the oxygen in the organic fraction of the coal is probably bound to hydrogen (as well as carbon), the depths of the 1.9 and 2.9 μm bands are an indication of the total hydrogen-bonded oxygen content., reflecting the fact that the majority of the oxygen in the samples is present in the inorganic phases. A number of investigators [28, 43–45,81,82] have also used small changes in the intensities of various oxygen-associated bands to track

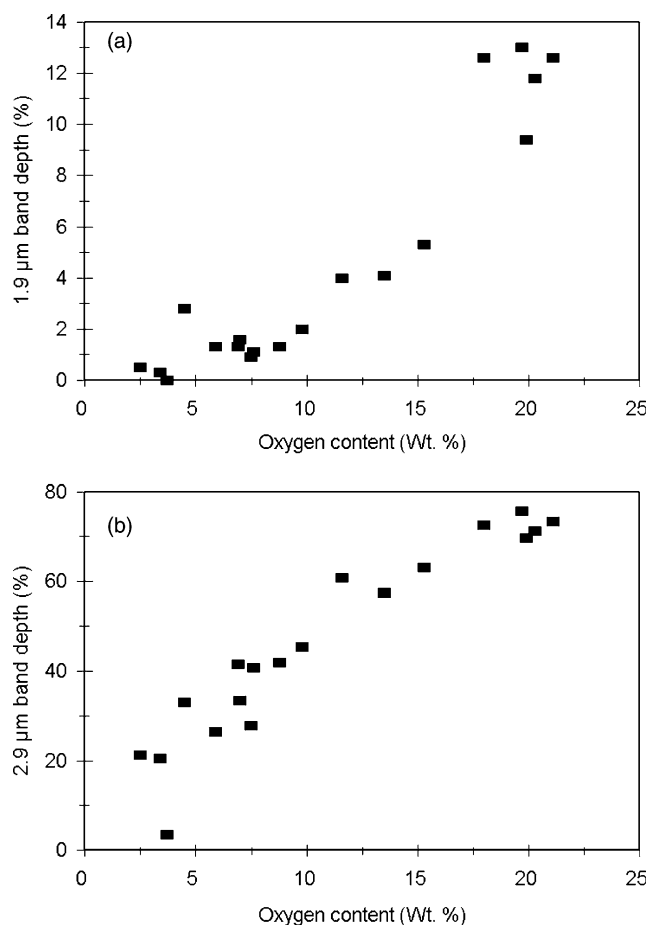


Fig. 14. Oxygen content versus: (a) depth of the absorption band near 1.9 μm (measured relative to a straight line continuum tangent to the reflectance spectrum on either side of this feature); (b) depth of the 2.9 μm absorption band measured relative to the local reflectance maximum in the 2.5–2.7 μm region.

oxidation and unravel oxidation pathways; however, the expected magnitude of these band variations as a function of oxygen content and other confounding spectral–compositional effects suggests that this approach, while appropriate for tracking oxidation effects, is not suitable for deriving total oxygen content. The ability to derive oxygen content in the organic phases is complicated by the fact that the ratios of oxygen-bearing species vary as a function of rank [83]. Partial least squares regression analysis has been used to correlate changes in spectral properties with the oxygen content of peat [35].

#### 4.15. Sulphur (wt%)

Sulphur in coals may be present in a number of forms including sulphides and in the organic phase [84]. Sulphur-associated absorption bands are generally weaker than those associated with other atoms. When coupled with the fact that coals generally contain low abundances of sulphur (usually on the order of a few percent or less), sulphur content determination using reflectance spectroscopy is

unlikely to yield useful results. The only evidence for sulphur-related spectral features in the reflectance spectra is a very weak band near 3.97 μm found in the sample with the highest sulphur abundance (4.83 wt.%). This band is in the region expected for S–H stretching vibrations and does not appear in the other coal spectra.

#### 4.16. H/C ratio

The H/C ratio obtained from ultimate analyses is strongly correlated with aromaticity [85], and hence should be most highly correlated with aliphatic and aromatic organic absorption bands. This is in fact the case; the best positive correlations were found with the depth of the 3.41 μm aliphatic absorption feature and the ratio of the 3.41/3.28 μm band depths (Fig. 15). This is consistent with previous studies which found correlations between aliphatic band intensities in transmission spectra and H/C ratios [37, 39,86]. There was also a general increase in absolute reflectance at 1.6 μm with increasing H/C ratio. Once again, much of the scatter in the data is probably attributable to the fact that the reflectance spectra are more sensitive to

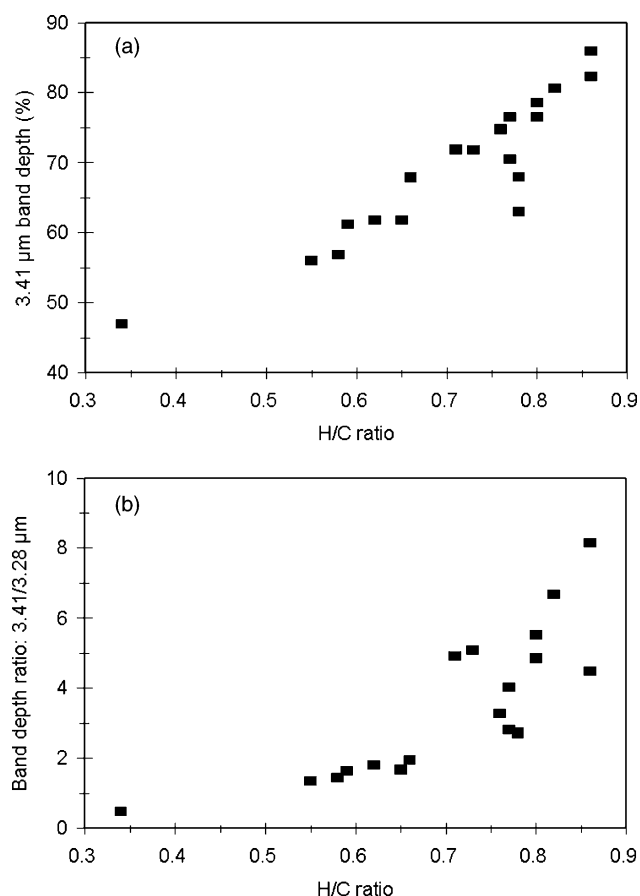


Fig. 15. H/C ratio versus: (a) depth of the absorption band at 3.41 μm (measured relative to the local reflectance maximum in the 2.5–2.7 μm region); (b) ratio of the depths of the 3.41/3.28 μm absorption bands measured relative to a straight line continuum tangent to the reflectance spectra on either side of these features.

the speciation of elements rather than overall elemental abundances. The fact that these correlations exist is due to the fact that the overall structures of the coal samples in terms of H–C configurations are all broadly similar. McCartney and Ergun [87] found a negative correlation between H/C ratio of vitrinites and their mean reflectance. A similar negative correlation was found between H/C ratio in the current samples and absolute reflectance at 0.4  $\mu\text{m}$ . However, the scatter in the data precludes the use of this correlation for quantitative determinations. This is probably due to the fact that the reflectance spectra of the whole rock samples do not discriminate between vitrinite and other H- and C-bearing components which can affect overall reflectance.

#### 4.17. Vitrinite mean reflectance

Vitrinite mean reflectance is positively correlated with coal rank, and hence carbon content. As was the case with carbon content correlations, the best correlations are found between mean vitrinite reflectance and depth of the 3.41  $\mu\text{m}$  band (negative correlation), and the 3.41/3.28  $\mu\text{m}$  band depth ratio (positive correlation) (Fig. 16). There are also positive correlations with absolute reflectances at both 0.4 and 1.6  $\mu\text{m}$ , although not as highly correlated as the former parameters.

#### 4.18. Calorific value

Calorific value is a complex function of elemental composition and hence is not expected to be directly derivable from analysis of reflectance spectra. The only correlations which were found for calorific value are with the ratio of the depth to absolute reflectance of the 3.28  $\mu\text{m}$  (aromatic) band (Fig. 17). The correlations are not strong enough to permit the use of these correlations for more than gross estimates of calorific value, however. Partial least squares regression analysis has been used to correlate changes in spectral properties with the calorific value of peat [35,48].

#### 4.19. Petrofactor

Petrofactor is a parameter which combines maceral and rank data in order to better relate coal properties to reactivity. It is the ratio of the mean reflectance to the sum (in wt%) of the vitrinite, (huminite in the case of low rank coals), exinite, (or liptinite) and one third of semi-fusinite (with the ratio multiplied by 1000) [36,88]. As this parameter increases with increasing mean vitrinite reflectance and vitrinite and liptinite content, it is expected to be positively correlated with spectral parameters related to aromatic content and rank. This is in fact the case; petrofactor is negatively correlated with depth of the 2.31  $\mu\text{m}$  (aliphatic) absorption feature, absolute reflectances at 0.4 and 1.6  $\mu\text{m}$ , and ratio of the 3.41/3.28  $\mu\text{m}$  absorption

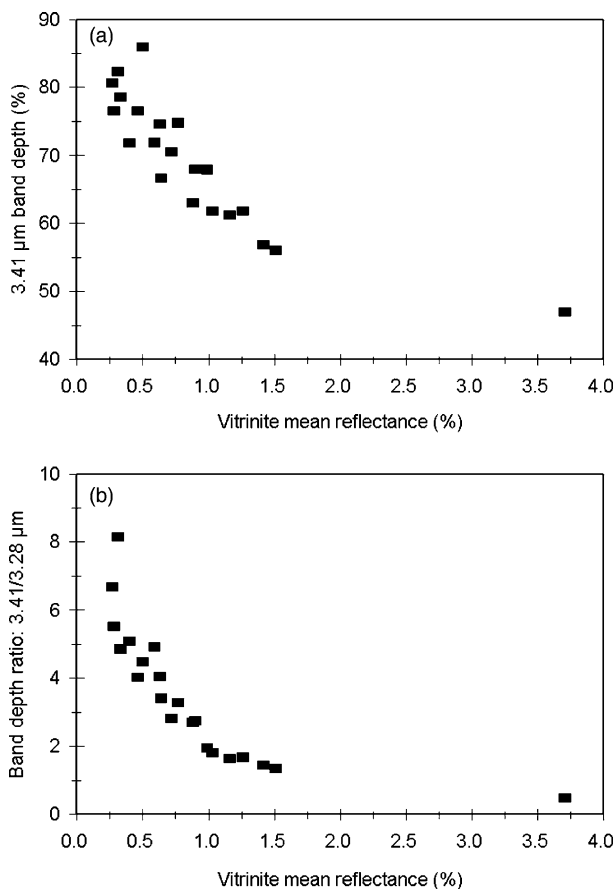


Fig. 16. Vitrinite mean reflectance versus: (a) depth of the absorption band at 3.41  $\mu\text{m}$  (measured relative to the local reflectance maximum in the 2.5–2.7  $\mu\text{m}$  region); (b) ratio of the depths of the 3.41/3.28  $\mu\text{m}$  absorption bands measured relative to a straight line continuum tangent to the reflectance spectra on either side of these features.

bands (Fig. 18). Once again, because petrofactor is a function of a number of coal parameters which are not explicitly expressed in the reflectance spectra, it should be applied judiciously.

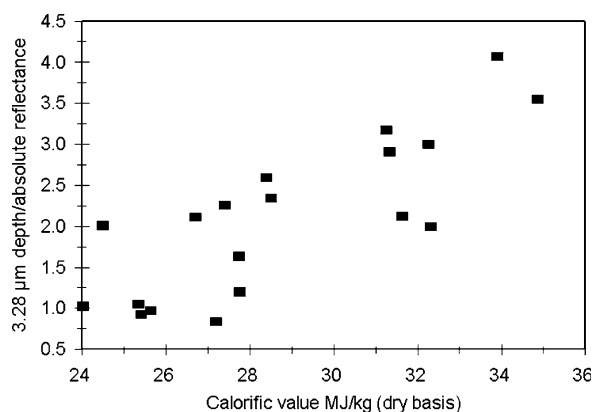


Fig. 17. Calorific value versus ratio of the depth of the absorption band at 3.28  $\mu\text{m}$  (measured relative to a straight line continuum tangent to the reflectance spectrum on either side of this feature) to the absolute reflectance of this band.

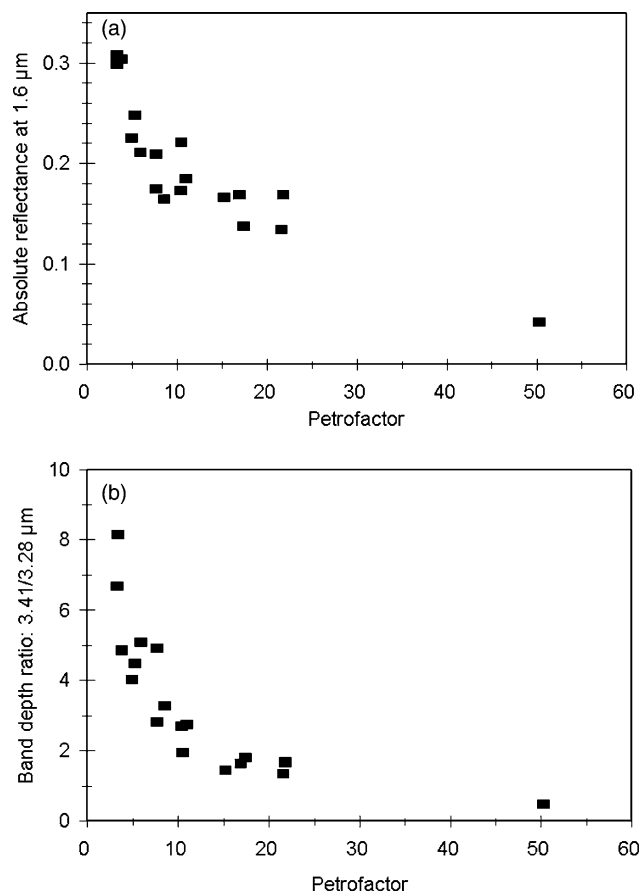


Fig. 18. Petrofactor versus: (a) absolute reflectance at 1.6  $\mu\text{m}$ ; (b) ratio of the depths of the 3.41/3.28  $\mu\text{m}$  absorption bands measured relative to a straight line continuum tangent to the reflectance spectra on either side of these features.

#### 4.20. Ignition temperature

Ignition temperature, defined as the temperature at which a 1% weight loss of the original coal occurs [36], has been found to be correlated with spectrally derivable parameters such as mean vitrinite reflectance, petrofactor, and H/C ratio. As these are derivable from the reflectance spectra (as described above), ignition temperature is similarly derivable from the reflectance spectra. However, given that ignition temperatures were only available for some of the samples, this relationship could not be derived for the total sample suite.

### 5. Effects of grain size variations

The coal samples which were examined for spectral–compositional relationships were of a consistent grain size ( $< 45 \mu\text{m}$ ) in order to minimize the spectrum-altering effects of grain size variations. In order to better characterize these variations a series of grain size separates of COAL16 ( $< 37$ , 37–63, 63–125, 125–250, 250–500, 500–1000 and 1000–2000  $\mu\text{m}$ ) were characterized (Fig. 19). All of the key spectral parameters such as absolute reflectances, band depths, and

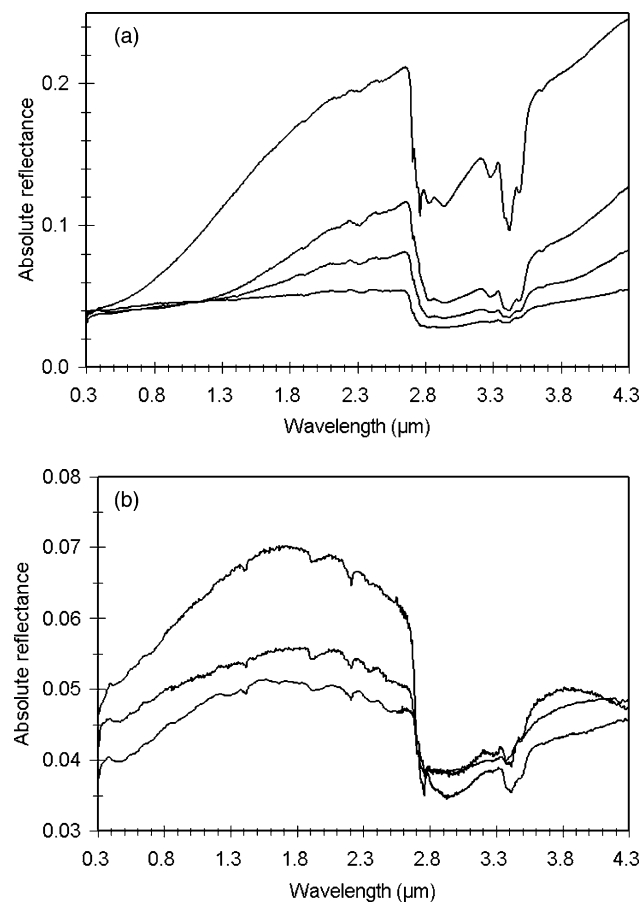


Fig. 19. Reflectance spectra (0.3–4.3  $\mu\text{m}$ ) of different size fractions of COAL16: (a) from top to bottom:  $< 37$ , 37–63, 63–125, 125–250  $\mu\text{m}$  fractions; (b) from top to bottom: 1000–2000, 250–500, 500–1000  $\mu\text{m}$  fractions.

band depth ratios varied as a function of grain size. However, none of these variations was consistent across the entire range of grain sizes examined. All of the spectral parameters examined showed both decreases and increases across the range of grain sizes examined. These results suggest that the derived spectral–compositional relationships are only strictly applicable for a consistent size fraction.

### 6. Discussion

The approach taken in this study is to focus on the use of absorption band depths or intensities rather than areas and to concentrate on simple spectral parameters such as band depths or ratios. The main reason for this is that in many instances individual absorption bands are highly overlapped, creating difficulties in determining individual band areas. Absorption bands are wider in reflectance than transmittance [89]. Band areas have been used successfully in the past to determine functional group abundances in coals from transmission spectra [26]. Infrared transmission spectroscopy is a very useful tool for determining the presence of specific functional groups and for studying the nature of

various types of atomic bonds [24,25]. More sophisticated spectral deconvolution algorithms, such as multivariate analysis, can be used for more detailed structural analysis [35,90,91] and for derivation of hydrocarbon properties [92] but the complexity and limitations of coal reflectance spectra makes this a non-trivial task.

With increasing rank, resolvable absorption bands in the 0.3–2.5  $\mu\text{m}$  region decrease in intensity until, in the case of anthracites, no resolvable absorption bands are present in this wavelength region [16]. In these cases, fundamental absorption bands, which are more intense than the shorter wavelength combination and overtone bands must be used for quantitative analysis.

This study, as well as previous studies [37] have shown that multiple compositional properties can often be derived from a single spectral parameter (Table 2). This arises from the fact that many coal properties are highly correlated [36, 37,85,93,94]. If these relationships are violated, then spectral analysis may only be justified for determination of the property which is directly expressed in the reflectance spectrum (e.g. aromatic content from depth of the 3.28  $\mu\text{m}$  aromatic absorption band). A number of studies [23,36] have shown that such spectral–compositional parameters cannot properly interpret ‘anomalous’ coals.

This multiple interdependency also provides some advantages for applying spectroscopy to coal analysis because it allows for the derivation of coal properties which are not directly derivable from absorption band properties, such as rank, calorific value, or vitrinite reflectance [23,36,37]. Consequently, the tractable compositional properties are not necessarily limited by the number of resolvable spectral features. In addition, spectrally derivable coal properties can be combined to yield more complex indices of coal properties [95]. While this study has focused on the correlations which exist between specific absorption features and specific coal properties, alternative approaches, based on techniques such as principal components regression of diffuse reflectance spectra, have also been found to yield good correlations for various coal properties [96]. In addition, more detailed analysis of coal and other hydrocarbon spectra can be used to elucidate structural variations which affect functional group absorption bands [30]. Some derived spectral–compositional correlations may be fortuitous and hence should be used with caution. As an example, H/C ratio, which is weakly correlated with some organic phase-associated spectral features, is reflecting the H/C ratio in the organic phase rather than in the whole rock sample. Thus, the usefulness of all spectral–compositional correlations should be assessed on the basis of what the applied spectral parameters are actually measuring.

As discussed above, most of the coal spectra exhibit distinct OH-associated absorption bands in the 2.7–2.8  $\mu\text{m}$  region which are attributable to specific clay minerals present in the samples. The positions and intensities of these bands could be used to identify

Table 2  
Strongest spectral–compositional correlations for coals

Coal property	Spectral correlation
Aromaticity factor	3.41 $\mu\text{m}$ absorption band depth (–) 3.41/3.28 $\mu\text{m}$ absorption bands depth ratio (–)
Aliphatic (CH + CH <sub>2</sub> + CH <sub>3</sub> ) content	3.41 $\mu\text{m}$ absorption band depth (+) 3.41/3.28 $\mu\text{m}$ absorption bands depth ratio (+)
Aromatic C content	3.41/3.28 $\mu\text{m}$ absorption bands depth ratio (–) 3.28 $\mu\text{m}$ absorption band depth: absolute reflectance ratio (+)
Moisture content	1.9 $\mu\text{m}$ absorption band depth (+) 2.9 $\mu\text{m}$ absorption band depth (+)
Volatile content	2.31 $\mu\text{m}$ absorption band depth (+) 3.41 $\mu\text{m}$ absorption band depth (+) 3.41/3.28 $\mu\text{m}$ absorption bands depth ratio (–)
Fixed carbon content	3.41 $\mu\text{m}$ absorption band depth (–) 3.41/3.28 $\mu\text{m}$ absorption bands depth ratio (–) 3.28 $\mu\text{m}$ absorption band depth: absolute reflectance ratio (+)
Fuel ratio	3.41/3.28 $\mu\text{m}$ absorption bands depth ratio (–) 2.31/3.28 $\mu\text{m}$ absorption bands depth ratio (–)
Carbon content	3.28 $\mu\text{m}$ absorption band depth: absolute reflectance ratio (+) 3.41/3.28 $\mu\text{m}$ absorption bands depth ratio (–)
Hydrogen content	3.41 $\mu\text{m}$ absorption band depth: absolute reflectance ratio (+) 2.9 + 3.41 $\mu\text{m}$ absorption band depths (+)
Nitrogen content	7.26 $\mu\text{m}$ absorption band depth (+)
Oxygen content	1.9 $\mu\text{m}$ absorption band depth (+) 2.9 $\mu\text{m}$ absorption band depth (+)
H/C ratio	3.41 $\mu\text{m}$ absorption band depth (+) 3.41/3.28 $\mu\text{m}$ absorption bands depth ratio (+)
Vitrinite mean reflectance	3.41 $\mu\text{m}$ absorption band depth (–) 3.41/3.28 $\mu\text{m}$ absorption bands depth ratio (–)
Calorific value	3.28 $\mu\text{m}$ absorption band depth: absolute reflectance ratio (+)
Petrofactor	Absolute reflectance at 1.6 $\mu\text{m}$ (–) 3.41/3.28 $\mu\text{m}$ absorption bands depth ratio (–)

Sign in brackets indicates the sign of the correlation.

the particular species which are present [66]. The use of coal spectra to determine the presence and abundance of specific minerals is beyond the scope of this current paper. However, this capability has been demonstrated using transmission spectra [39,97,98].

The correlations derived from this study are strictly only applicable to < 45  $\mu\text{m}$  grain size fractions. Increasing the grain size of the sample can cause spectral parameters such as band depths, absolute reflectances, and band depth ratios to exhibit non-systematic variations. These variations are probably the result of changes in the ratio of surface to volume scattering as a function of grain size, which will

vary depending on the optical properties of the sample at specific wavelengths [70]. As an example, an initial increase in band depth with increasing grain size, followed by a decrease in band depth could be due to band saturation [65].

The results derived from this study suggest that reflectance spectroscopy could be applied to on-line monitoring of coal properties in a process stream. Such a capability has been demonstrated for oil sands [99,100]. On-line FTIR (non-reflectance) analysis has also been applied to coal characterization [22], and the results of this study suggest that diffuse reflectance infrared spectroscopy could supplant or complement these techniques for rapid quantitative coal characterization.

### Acknowledgements

This study was supported by research grants from Imperial Oil Limited, the Petroleum Research Fund of the American Chemical Society and the University of Winnipeg. Thanks to Dr Wolfgang Kalkreuth of the Institute of Sedimentary and Petroleum Geology of the Geological Survey of Canada for providing a number of the samples used in this study, and to Drs Carlé Pieters and Takahiro Hiroi for acquisition of the reflectance spectra at the NASA-funded multi-user RELAB facility in the Department of Geological Sciences at Brown University. Thanks also to the two anonymous reviewers for their cogent comments.

### References

- [1] Hayatsu R, Scott RG, Moore LP, Studier MH. *Nature* 1975;257:378.
- [2] Davidson RM. Molecular structure of coal. Report No. ICTIS/TR 08. IEA Coal Research; 1980.
- [3] Haenel MW. *Fuel* 1992;71:1211.
- [4] Karr JrC. Analytical methods for coal and coal products. New York: Academic Press; 1978.
- [5] Speight JG. Analytical methods for coal and coal products, vol. II. New York: Academic Press; 1978. p. 75–99.
- [6] Parus J, Kierzek J, Małozewska-Bućko B. *X-ray Spectrom* 2000;29:192–5.
- [7] Cannon CG, Sutherland GBBM. *Trans Faraday Soc* 1945;41:279.
- [8] Friedel RA. *Applied infrared spectroscopy*. New York: Reinhold; 1966. p. 312–43.
- [9] Fuller MP, Hamadeh IM, Griffiths PR, Lowenhaupt DM. *Fuel* 1982;61:529.
- [10] Ito O, Seki H, Iino M. *Fuel* 1988;67:573.
- [11] Christy AA, Dahl B, Kvalheim OM. *Fuel* 1989;68:430.
- [12] Fuller Jr EL, Smyrl NR. *Appl Spectrosc* 1990;44:451.
- [13] Mastalerz M, Bustin RM. *Fuel* 1995;74:536.
- [14] Vidrine DW. *Appl Spectrosc* 1980;34:314.
- [15] Donini JC, Michaelian KH. *Infrared Phys* 1986;26:135.
- [16] McAskill NA. *Appl Spectrosc* 1987;41:313.
- [17] Blob AK, Rullkötter J, Welte DH. *Org Geochem* 1987;13:1073.
- [18] Rochdi A, Landais P. *Fuel* 1991;70:367.
- [19] Ruau O, Landais P, Gardette JL. *Fuel* 1997;76:645.
- [20] Thomasson J, Coin C, Kahraman H, Fredericks PM. *Fuel* 2000;79:685.
- [21] Mielczarski JA, Deńca A, Strojek JW. *Appl Spectrosc* 1986;40:998.
- [22] Solomon PR. *Advances in coal spectroscopy*. New York: Plenum Press; 1992. p. 341–71.
- [23] Iglesias MJ, Jiménez A, Laggoun-Défarge F, Suárez-Ruiz I. *Energy Fuels* 1995;9:458.
- [24] Friedel RA, Retcofsky HL, Queiser JA. *Adv Coal Spectrom; Bur Mines Bull* 1967;640.
- [25] Painter P, Starsinic M, Coleman M. *Fourier transform infrared spectroscopy, vol. 4. Applications to chemical systems*. New York: Academic Press; 1985. p. 169–241.
- [26] Martin KA, Chao SS. *Prepr—Fuel Chem Div, Am Chem Soc* 1988;33(3):17.
- [27] Dela Rosa L, Pruski M, Lang D, Gerstein B, Solomon P. *Energy Fuels* 1992;6:460.
- [28] Verheyen TV, Johns RB, Esdaile RJ. *Geochim Cosmochim Acta* 1983;47:1579.
- [29] Solomon PR, Carangelo RM. *Fuel* 1988;67:949.
- [30] Černý J. *Fuel* 1996;75:1301.
- [31] Friedel RA, Queiser JA. *Fuel* 1959;38:369.
- [32] Cloke M, Gilfillan A, Lester E. *Fuel* 1997;76:1289.
- [33] Bodoev NV, Guet JM, Gruber R, Dolgopov NI, Wilhelm JC, Bazarova O. *Fuel* 1996;75:839.
- [34] D'Alessio A, Vergamini P, Benedetti E. *Fuel* 2000;79:1215.
- [35] Holmgren A, Nordén B. *Appl Spectrosc* 1988;42:255.
- [36] Furimsky E, Palmer AD, Kalkreuth WD, Cameron AR, Kovacik G. *Fuel Process Technol* 1990;25:135.
- [37] Kalkreuth W, Steller M, Wieschenkämper I, Ganz S. *Fuel* 1991;70:683.
- [38] Ganz H, Kalkreuth W. *Fuel* 1987;66:708.
- [39] Ganz HH, Kalkreuth W. *J Southeast Asian Earth Sci* 1991;5:19.
- [40] Rowan LC, Salisbury JW, Kingston MJ, Vergo N, Bostick NH. *J Geophys Res* 1991;96:18047.
- [41] Gilbert LA. *Fuel* 1960;39:393.
- [42] Ito O. *Energy Fuels* 1992;6:662.
- [43] Goodarzi F, Murchison DG. *Fuel* 1973;52:90.
- [44] Gethner JS. *Appl Spectrosc* 1987;41:50.
- [45] Fuller Jr EL, Smyrl NR. *Prepr—Fuel Chem Div, Am Chem Soc* 1988;33:691.
- [46] Machnikowska H, Krztoń A, Machnikowski J. *Fuel* 2002;81:245.
- [47] Fredericks PM, Kobayashi R, Osborn PR. *Fuel* 1987;66:1603.
- [48] Johansson E, Persson JA, Albano C. *Fuel* 1987;66:22.
- [49] Rowan LC, Poole FG, Pawlewicz MJ. *AAPG Bull* 1995;79:1464.
- [50] Tosi C, Pinto A. *Spectrochim Acta* 1972;28A:585.
- [51] Vorres KS. *User handbook for the Argonne premium coal sample program. ANL/PCSP-93/1*, Argonne, IL: Argonne National Laboratory; 1993.
- [52] Fuller Jr EL, Smyrl NR. *Fuel* 1985;64:1143.
- [53] Sobkowiak M, Painter P. *Energy Fuels* 1995;9:359.
- [54] Yang CQ, Simms JR. *Fuel* 1995;74:543.
- [55] Cloutis EA. *Science* 1989;245:165.
- [56] Cloutis EA. *AOSTRA J Res* 1990;6:17.
- [57] Cloutis EA, Gaffey MJ, Moslow TF. *Icarus* 1994;107:276.
- [58] Cloutis EA, Gaffey MJ, Moslow TF. *Fuel* 1995;74:874.
- [59] Bishop JL, Koeberl C, Kralik C, Fröschl H, Englert PAJ, Andersen DW, Pieters CM, Wharton Jr RA. *Geochim Cosmochim Acta* 1996;60:765.
- [60] Pieters CM. *J Geophys Res* 1983;88:9534.
- [61] RELAB, *Reflectance experiment laboratory (RELAB) description and user's manual*. Providence, RI: Brown University; 1996.
- [62] Weidner VR, Hsia JJ. *J Opt Soc Am* 1981;71:856.
- [63] Clark RN, Roush TL. *J Geophys Res* 1984;89:6329.
- [64] Fysh SA, Swinkels DAJ, Fredericks PM. *Appl Spectrosc* 1985;39:354.
- [65] Hunt GR, Salisbury JW. *Mod Geol* 1970;1:283.
- [66] Clark RN, King TVV, Klejwa M, Swayze GA. *J Geophys Res* 1990;95:12653.

- [67] Cannon CG, George WH. Proceedings of a Conference on the Ultra-Fine Structure of Coals and Cokes. British Coal Utilization Research Association; 1944. p. 290–315.
- [68] Gavrilov MZ, Ermolenko IN. *J Appl Spectrosc* 1975;23:955.
- [69] Painter PC, Sobkowiak M, Youtcheff J. *Fuel* 1987;66:973.
- [70] Salisbury JW, Walter LS. *J Geophys Res* 1989;94:9192.
- [71] Jenkins RG, Walker JrPL. Analytical methods for coal and coal products. New York: Academic Press; 1978. p. 265–92.
- [72] Supaluknari S, Larkins FP, Redlich P, Jackson WR. *Fuel Process Technol* 1989;23:47.
- [73] Brown JK. *J Chem Soc* 1955;(1955):744.
- [74] Chen C, Gao J, Yan Y. *Energy Fuels* 1998;12:446.
- [75] Vassilev SV, Vassileva CG. *Fuel Process Technol* 1996;48:85.
- [76] Vassilev SV, Kitano K, Vassileva CG. *Fuel* 1996;75:1537.
- [77] Estep PA, Kovach JJ, Karr Jr C. *Anal Chem* 1968;40:358.
- [78] Axelson DE. *Fuel Process Technol* 1987;16:257.
- [79] Berkowitz N. An introduction to coal technology. New York: Academic Press; 1997.
- [80] Silverstein RM, Bassler GC, Morrill TC. Spectrometric identification of organic compounds, 5th ed. New York: Wiley; 1991.
- [81] Smyrl NR, Fuller JrEL. Coal and coal products: analytical characterization techniques. American Chemical Society; 1982. p. 133–45.
- [82] Lynch BM, Lancaster LI, MacPhee JA. *Fuel* 1987;66:979.
- [83] Winans RE, McBeth RL, Melnikov PE, Botto RE. *Proc Seventh Int Conf Coal Sci* 1993;II:515–8.
- [84] Huffman GP, Mitra S, Huggins FE, Shah N, Vaidya S, Lu F. *Energy Fuels* 1991;5:574.
- [85] Maroto-Valer MM, Love GD, Snape CE. *Fuel* 1994;73:1926.
- [86] Ballice L, Yüksel M, Saglam M, Schulz H, Hanoglu C. *Fuel* 1995;74:1618.
- [87] McCartney JT, Ergun S. Optical properties of coals and graphite. US Department of the Interior, Bureau of Mines Bulletin; 1967.
- [88] Diessel K, Guyot E. Proceedings of the Ninth International Congress on Stratigraphy and Geology of the Carboniferous; 1979. p. 573.
- [89] Cloutis EA, Bell III JF. *J Geophys Res* 2000;105:7053.
- [90] Painter PC, Snyder RW, Starsinic M, Coleman MM, Kuehn DW, Davis A. *Appl Spectrosc* 1981;35:475.
- [91] Kroo E, Bonanno AS, Serio MA, Solomon PR. Proceedings of the Seventh International Conference on Coal Science; 1993. p. 473–6.
- [92] Fodor GE, Kohl KB, Mason RL. *Anal Chem* 1996;68:23.
- [93] Maroto-Valer MM, Andrésen JM, Snape CE. *Fuel* 1998;77:792.
- [94] Bratek K, Bratek W, Gerus-Piasecka I, Jasieńko S, Wiik P. *Fuel* 2002;81:97.
- [95] Su S, Pohl JH, Holcombe D, Hart JA. *Fuel* 2001;80:699.
- [96] Alciaturi CE, Escobar ME, Vallejo R. *Fuel* 1996;75:491.
- [97] Ganz H. 13th International Meeting of Organic Geochemistry, Venezia, Italy. ; 1987. p. 251.
- [98] Ganz H, Kalkreuth W, Öner F, Pearson MJ, Small JS. Petroleum geology of North West Europe. London: Graham & Trotman; 1987. p. 847–51.
- [99] Dougan PD. *AOSTRA J Res* 1989;5:203.
- [100] Shaw RC, Kratochvil B. *Anal Chem* 1990;62:167.